Biochemical and Biophysical Research Communications **292,** 128–132 (2002)
doi:10.1006/bbrc.2002.6615, available online at http://www.idealibrary.com on IDEAL®

Phosphatase and Oxygen Radical-Generating Activities of Mammalian Purple Acid Phosphatase Are Functionally Independent

Helena Kaija,*,[1] Sari L. Alatalo,†,[1] Jussi M. Halleen,† Ylva Lindqvist,‡ Gunter Schneider,‡ H. Kalervo Väänänen,† and Pirkko Vihko*,[2]

**Biocenter Oulu, Research Center for Molecular Endocrinology, Oulu University Hospital, P.O. Box 5000, FIN-90014 University of Oulu, Finland; †Institute of Biomedicine, Department of Anatomy, Kiinanmyllynkatu 10, University of Turku, FIN-20520 Turku, Finland; and ‡Department of Medical Biochemistry and Biophysics, Karolinska Institutet, Scheelevägen 2, S-17177 Stockholm, Sweden*

Received February 13, 2002

Bone-resorbing osteoclasts and activated macrophages express large amounts of tartrate-resistant acid phosphatase (TRAP), an iron-containing enzyme with unknown biological function. We studied acid phosphatase (AcP) and reactive oxygen species (ROS)-generating activities of recombinant rat TRAP. pH optimum was 4.5 for AcP activity and 6.5 for ROS-generating activity. Replacement of His113 and His216 by site-directed mutagenesis severely inhibited AcP activity, but had no significant effects on ROS-generating activity. Substrate specificity was not affected by the mutations. These results suggest that AcP and ROS-generating activities of TRAP are functionally independent. © 2002 Elsevier Science (USA)

Key Words: **purple acid phosphatase; AcP; ROS; substrate specificity; site-directed mutagenesis.**

Mammalian tartrate resistant acid phosphatase (TRAP, EC 3.1.3.2) is a basic glycoprotein whose expression under physiological conditions is restricted to osteoclasts and activated macrophages, especially alveolar macrophages of the lung (1). Together with similar enzymes isolated from animals, plants and fungi, it belongs to the group of purple acid phosphatases (2). The physiological functions of purple acid phosphatases in biological systems are not yet known, and no natural substrates have been unambiguously established. Mice deficient in TRAP develop mild osteopetrosis (3), and overexpression of TRAP causes increased rate of bone turnover (4), suggesting that TRAP has an important role in bone resorption.

The catalytic site of TRAP contains a binuclear iron center, where one of the irons is redox-active, while the other is in the ferric state (5). The enzyme may exist in two forms: the inactive purple form, where the redox-active iron is in the ferric state, and the active pink form, where it is reduced to the ferrous state. The active enzyme is also capable of generating reactive oxygen species (ROS) through Fenton's reaction, where the ferrous ion reacts with hydrogen peroxide to produce highly destructive hydroxyl radicals (6–8). Thus, the same active site is used for both the acid phosphatase (AcP) and the ROS-generating activity, and both activities require the redox-active iron to be in the ferrous form.

The binuclear iron center of purple acid phosphatases has been studied extensively using various spectroscopic techniques (5, 9–11). More recently, the crystal structures of mammalian (12–14) and plant (15, 16) purple acid phosphatases have been determined. The crystallographic studies have revealed that the highly conserved residues His113, His216, and Asp267 line the active-site cleft of the mammalian enzyme, and these amino acids have therefore been implicated in substrate binding and/or catalysis. In this work, we have probed the proposed role of these residues in the enzymatic mechanism of rat purple acid phosphatase using site-directed mutagenesis.

MATERIALS AND METHODS

Site-directed mutagenesis. Site-directed mutagenesis was achieved by using the QuikChange site-directed mutagenesis kit (Stratagene, West Cedar Creek, TX). This method allows site-directed mutation in double-stranded plasmid (17). The following oligonucleotide primers were used to generate the desired mutations: D267A, 5′-GGCAACTTCATGGCCCCTTCTGTGCGG-3′ and 5′-CCGCACAGAAGGGGCCATGAAGTTGCC-3′, H216A, 5′-CCCATCTGGTCCATCGCCGAGGCCGGACCCACCCGCTGCCTGGTC-3′ and 5′-GACCAGGCAGCGGGT-

[1] These authors contributed equally to this work.

[2] To whom correspondence and reprint requests should be addressed. Fax: +358-8-3155631. E-mail: pvihko@whoccr.oulu.fi.

0006-291X/02 $35.00

GGGTCCGGCCTCGGCGATGGACCAGATGGG-3′, H216Q, 5′-CCCATCTGGTCCATCGCCGAGCAGGGACCCACCCGCTGCCTGGTC-3′ and 5′-GACCAGGCAGCGGGTGGGTCCCTGCTCGGCGATGGACCAGATGGG-3′, H113A, 5′-GTGCTGGCTGGAAACGCTGATCACCTTGGCAATGTC-3′ and 5′-GACATTGCCAAGGTGATCAGCGTTTCCAGCCAGCAC-3′, H113Q, 5′-GTGCTGGCTGGAAACCAAGATCACCTTGGCAATGTC-3′ and 5′-GACATTGCCAAGGTGATCTTGGTTTCCAGCCAGCAC-3′. The transfer vector pVL1392, which contains the rat bone TRAP DNA fragment was used as the template (18). The mutation products were sequenced using the ABI PRISM BigDye Terminator Cycle Sequencing Ready Reaction kit (Perkin–Elmer, Norwalk, CT) to verify the mutation and the integrity of the rest of DNA.

Enzyme production and purification. The wild-type and mutant proteins were produced in *Sf* 9 insect cells (19) and purified to apparent homogeneity with the methods published earlier (18). The purity of the mutant proteins was evaluated by SDS–PAGE (20) using PhastSystem (Pharmacia, Uppsala, Sweden) with PhastGel gradient media 10-15. Protein concentrations were measured according to the Bradford method (21). The replacement of Asp267 by alanine creates a possible additional glycosylation site in the enzyme. This variant however, showed no increase in the molecular mass when evaluated by SDS–PAGE electrophoresis.

Kinetic characterization of mutant enzymes. The formation of ROS was determined by monitoring the formation of malondialdehyde acetal from degradation products of deoxyribose (22). Substrate specificity was studied by measuring phosphatase activity as follows (23): 100 μl of 200 nM enzyme diluted in 50 mM sodium citrate buffer, pH 4.5, was reduced with 200 mM 2-mercaptoethanol. The reduced enzyme was incubated with 100 μl of 6.25 mM 4-nitrophenyl phosphate (4-NPP), β-glycerophosphate, *o*-phospho-L-serine and *o*-phospho-L-tyrosine, respectively, dissolved in the same buffer, for 15 min at 37°C. The reaction was terminated by the addition of 800 μl of ice-cold 3.75% trichloroacetic acid. The mixture was placed in an ice-water bath for 5 min. The denatured protein was pelleted by centrifugation for 3 min in an Eppendorf centrifuge. The reaction vials were immediately placed in an ice-water bath, and analysis of the released inorganic phosphate was performed on a 200-μl aliquot of the supernatant. 200 μl of sample, 800 μl of water, 200 μl of reagent A (2% ammonium molybdate · $4H_2O$), and 300 μl of reagent B (14% ascorbic acid in 50% trichloroacetic acid) were mixed and, after one m, 1 ml of reagent C (2% trisodium citrate · $2H_2O$ plus 2% sodium arsenite in 2% (v/v) acetic acid) was added. Color was allowed to develop for 4 min, and absorbance was measured at 700 nm.

In the kinetic measurements, 4-NPP was used as substrate. All measurements were carried out in triplicate. The following substrate concentrations were used: 0.8–200 mM for wild-type and mutant Asp267Ala, 0.8–50 mM for the mutants at position His216 and 0.8–100 mM at position His113. The steady-state kinetic constants for 4-NPP were derived from the analysis of rate vs substrate concentration. K_m and V_{max} values were calculated by nonlinear regression analysis using the GraphPrismPad software.

Absorption spectra. The absorption spectra were determined using 400 μg of purified non-reduced wild-type enzyme and the mutants Asp267Ala, His216Ala, His216Gln, His113Ala, and His113Gln in a total volume of 60 μl of 50 mM sodium acetate buffer at pH 5.0. The spectra were recorded with a Shimadzu UV 160-A spectrophotometer.

RESULTS

Kinetic Parameters and Substrate Specificity of AcP Activity

The K_m and V_{max} values of the wild-type and mutated enzymes with 4-NPP as substrate are shown in Table 1. The specific activity of the wild-type enzyme toward phosphotyrosine was comparable to the activity with 4-NPP. Phosphoserine and β-glycerophosphate, however, were not hydrolyzed by the wild-type enzyme nor by any of the mutants. The K_m values for 4-NPP were of the same order of magnitude for all mutants, with the largest decrease (about fivefold) occurring in the His113Gln and His216Ala mutants compared to the wild-type enzyme. Significant decreases in the k_{cat} values were seen for the mutants at the positions His113 and His216, where substitutions led to a drop in rate by up to two orders of magnitude. In terms of catalytic efficiency, the mutations at position 113 were most deleterious, with a drop in k_{cat}/K_m by up to 75-fold (His113Ala).

TABLE 1

Kinetic Parameters of Wild-Type and Mutant TRAP

Enzyme	K_m (mM)	k_{cat} (s^{-1})	k_{cat}/K_m (s^{-1} M^{-1})
Wild-type	40.6 ± 4.1	404.5 ± 19.9	$10.0 \times 10^3 \pm 0.38 \times 10^3$
D267A	47.9 ± 9.5	415.7 ± 58.6	$8.5 \times 10^3 \pm 0.61 \times 10^3$
H216A	6.1 ± 0.3	23.2 ± 4.5	$3.8 \times 10^3 \pm 0.56 \times 10^3$
H216Q	22.3 ± 3.4	15.0 ± 2.1	$0.7 \times 10^3 \pm 0.04 \times 10^3$
H113A	15.4 ± 0.1	2.4 ± 0.1	$0.2 \times 10^3 \pm 0.01 \times 10^3$
H113Q	6.7 ± 0.1	7.8 ± 3.6	$1.2 \times 10^3 \pm 0.50 \times 10^3$

Note. Measurements were carried out in 0.05 M Na-citrate buffer, pH 4.5, using 4-nitrophenyl phosphate as substrate. Values are means ± SD, $n = 3$.

The k_{cat}/K_m versus pH profiles of wild-type TRAP and the Asp267Ala mutant were very similar, and the catalytic efficiency of this mutant was not impaired significantly over the whole pH range measured (Fig. 1). The His216Ala mutant showed a shift in pH dependency and recovered to reach similar k_{cat}/K_m values as wild-type TRAP at very low pH values. Substitutions at the position His113 led to a mutant enzyme with very low catalytic efficiency over the whole pH range.

Comparison of AcP and ROS-Generating Activities

Figure 2A shows the rate versus pH curves for the AcP and ROS-generating activities of wild-type recombinant rat TRAP. The curves were different for the two reactions, with the pH optimum for phosphoester hydrolysis close to pH 4.5 and the pH optimum for ROS-generating activity at pH 6.5. To further determine if there are differences between the AcP and the ROS-generating activities of recombinant rat TRAP, we studied if the mutants at the positions His113 and His216, which were almost inactive as acid phosphatase, were able to generate ROS. As shown in Fig. 2B, the ROS-generating capacity was only slightly impaired in the four mutants. For both histidine residues, the mutation to alanine inactivated the ROS-generating activity more than the mutation to glutamine.

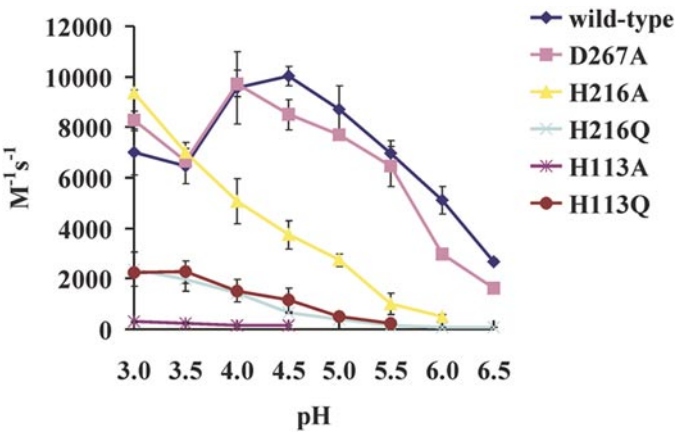

FIG. 1. k_{cat}/K_m versus pH profile for wild-type and mutant TRAP.

Absorption Spectra

The absorption maximum of the wild-type enzyme in the visible region of the spectrum was at 514 nm. The Asp267Ala mutant was slightly more oxidized, as indicated by the shift in the absorption maximum to 534 nm. The absorption maximum of all the other variants were at 507–514 nm (data not shown).

DISCUSSION

Rat purple acid phosphatase is a globular enzyme with overall dimensions of 36 × 42 × 54 Å (14). The structure consists of two seven-stranded mixed β-sheets, with each sheet flanked by solvent-exposed α-helices on one side. The two β-sheets pack onto each other, forming a β-sandwich. The binuclear iron center is located at the bottom of the active-site pocket at one edge of the β-sandwich. The highly conserved polar residues (Fig. 3) His113, His216, and Asp267, which are also conserved in the plant enzymes, line the active-site cleft. The replacement of the residues His216 and His113 by alanine seriously impaired the AcP activity of recombinant rat TRAP, which demonstrated that these two residues have an important role in phosphoester hydrolysis. The recovery of k_{cat}/K_m in the His216Ala mutant at low pH values suggests that this residue might also participate in leaving group protonation. The observed increase in k_{cat}/K_m at low pH might be due to direct protonation of the leaving group, which partly compensates for the loss of the proton-donating histidine side chain.

Our findings are consistent with most of the conclusions derived from crystallographic studies. The active site structures of mammalian (12–14) and plant purple acid phosphatase (15) revealed hydrogen bond interactions of His113 and His216 with oxygen atoms of bound phosphate. Thus, it was proposed that the positively charged imidazole side chains stabilize the negative charge developing at the oxygen atoms in the transition state (14, 16). Our findings also revealed that the role of Asp267 in catalysis suggested previously (14) seems less likely.

Our results further show that the AcP and the ROS-generating activities of TRAP are independent of each other. They have different pH optima, and the mutants of the enzyme that are almost inactive as acid phosphatase still have a high capacity to generate ROS. Although both of these two activities require the binuclear iron center, and especially the redox-active iron in the reduced state, the underlying catalytic mechanisms appear to be different. In AcP activity, a rather complex molecule with a phosphate group attached to an aromatic hydroxyl group binds to the active site, whereas in ROS-generating activity, the substrate is hydrogen peroxide, a much smaller molecule with a completely different structure. The present mutagenesis data indicate that different amino acids are important for the binding of these two substrates into the active site and the catalytic rate acceleration. The different pH optima of the two activities suggest that they

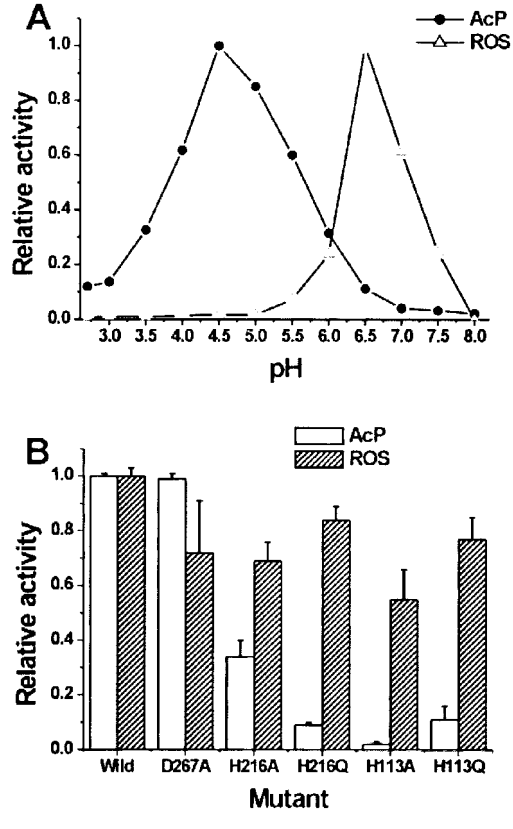

FIG. 2. Comparison of the phosphatase and radical-generating activities of wild-type and mutant rat TRAP. (A) pH optima of the two activities. The results are presented as relative activities, where the activities at the pH optima were given the value 1.0; (B) Comparison of the AcP and ROS-generating activities in the wild-type enzyme and in the mutated forms Asp267Ala, His113Ala, His113Gln, His216Ala, and His216Gln. Results are presented as relative specific activities, where the specific activities of the wild-type enzyme were given the value 1.0.

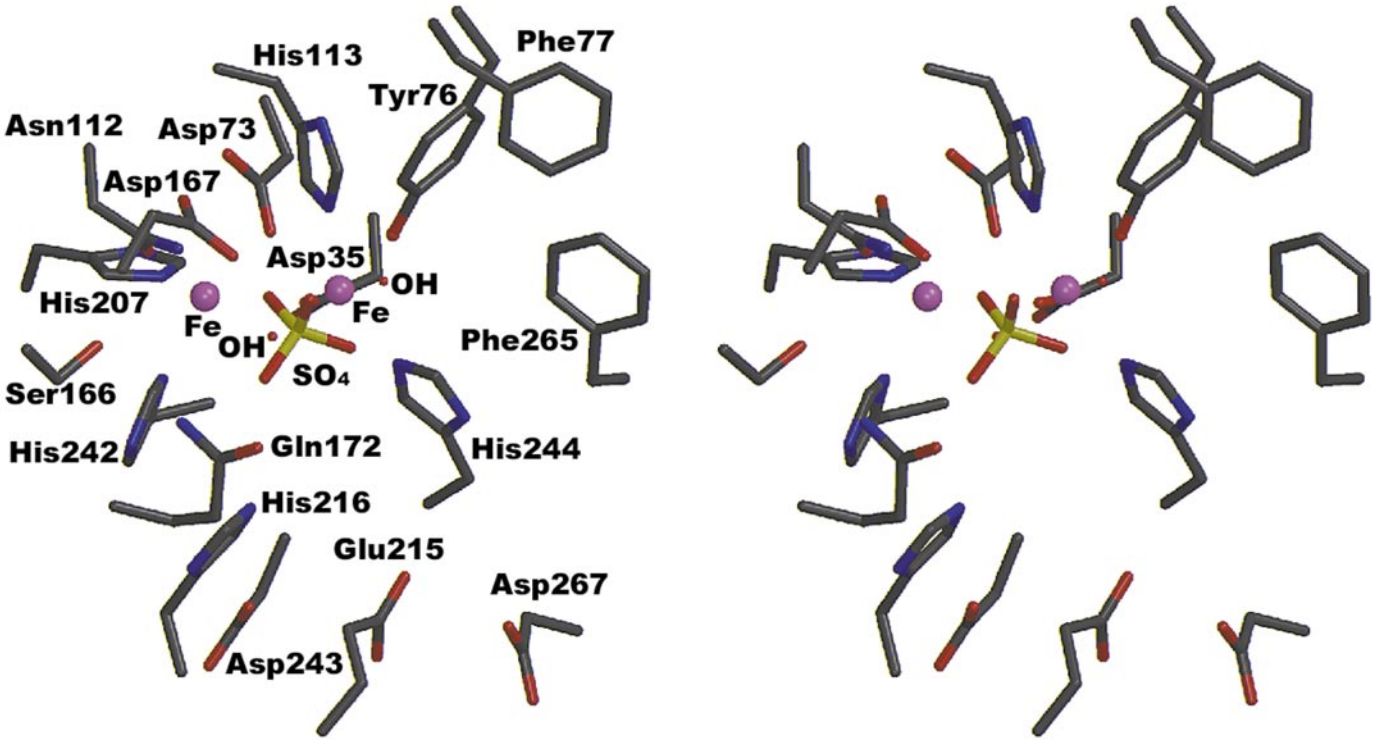

FIG. 3. Stereoview of the active site in purple acid phosphatase color-coded according to atom type. The bound sulfate ion indicates the approximate position of phosphate in the enzyme–P_i complex.

may be utilized in different intracellular compartments, and that the pH of the compartment may be one important determinant of which of the activities of this dual enzyme is most significant.

We and others have shown that TRAP is capable of hydrolyzing free and peptide-bound phosphotyrosine, but not phosphoserine. However, there are studies indicating that some phosphoserine-containing proteins, such as osteopontin and bone sialoprotein, may be useful substrates for this enzyme (24). These studies suggest that the AcP activity of TRAP would function in the resorption lacuna, which has an acidic pH.

Large amounts of TRAP are found in bone-resorbing osteoclasts and activated macrophages. In resorbing osteoclasts, TRAP is localized in transcytotic vesicles transporting bone matrix components from the resorption lacuna to a functional secretory domain in the basolateral membrane (8). The ROS generated by TRAP are capable of destroying type I collagen, the major protein in the bone matrix, and macrophages overexpressing TRAP have increased amounts of intracellular ROS (8).

Previous studies have shown that resorbing osteoclasts produce superoxide that is endocytosed from the ruffled border into an intracellular compartment (probably the transcytotic vesicles) containing superoxide dismutase, an enzyme that converts superoxide to hydrogen peroxide (25). Thus, the transcytotic vesicles of osteoclasts may contain large quantities of both superoxide and hydrogen peroxide, which are important substrates for the continuous production of ROS by TRAP. Hydrogen peroxide is needed to produce ROS by Fenton's reaction and superoxide to convert the redox-active iron of TRAP back into the ferrous form, thereby maintaining the mixed-valent form needed to produce ROS.

In activated macrophages, TRAP is localized in the antigen presentation route transporting endocytosed foreign material into the cell membrane where they are presented to other cells of the immune system (26). Both the transcytotic route of osteoclasts and the antigen presentation route of macrophages represent a transport route from a late endosomal/lysosomal compartment to the cell membrane, and it would be reasonable to suggest that TRAP would have a similar biological function in these analogous intracellular routes. This function could be to generate ROS that would be used to further destroy the initial bone matrix degradation products in the transcytotic vesicles of osteoclasts and the foreign antigens in the antigen presentation route of macrophages.

ACKNOWLEDGMENTS

We thank Marja-Riitta Hurnasti, Marja-Liisa Norrena, and Pirkko Ruokojärvi for their skillful technical assistance. This work was supported by the Research Council of the Academy of Finland, the State Technology Development Center of Finland (TEKES), the

Sigrid Juselius Foundation, the Graduate School of Musculoskeletal Diseases (TULES), and the Swedish Research Council—Medical Sciences.

REFERENCES

1. Yaziji, H., Janckila, A. J., Lear, S. C., Martin, A. W., and Yam, L. T. (1995) Immunohistochemical detection of tartrate-resistant acid phosphatase in non-hematopoietic human tissues. *Am. J. Clin. Pathol.* **104,** 397–402.
2. Vincent, J. B., Crowder, M. W., and Averill, B. A. (1992) Hydrolysis of phosphate monoesters: A biological problem with multiple chemical solutions. *Trends Biochem. Sci.* **17,** 105–110.
3. Hayman, A. R., Jones, S. J., Boyde, A., Foster, D., Colledge, W. H., Carlton, M. B., Evans, M. J., and Cox, T. M. (1996) Mice lacking tartrate-resistant acid phosphatase (Acp 5) have disrupted endochondral ossification and mild osteopetrosis. *Development* **122,** 3151–3162.
4. Angel, N. Z., Walsh, N., Forwood, M. R., Ostrowski, M. C., Cassady, A. I., and Hume, D. A. (2000) Transgenic mice overexpressing tartrate-resistant acid phosphatase exhibit an increased rate of bone turnover. *J. Bone Miner. Res.* **15,** 103–110.
5. Doi, K., Antanaitis, B. C., and Aisen, P. (1988) The binuclear iron centers of uteroferrin and the purple acid phosphatase. *Struct. Bonding* **70,** 1–26.
6. Hayman, A. R., and Cox, T. M. (1994) Purple acid phosphatase of the human macrophage and osteoclast. Characterization, molecular properties, and crystallization of the recombinant di-iron-oxo protein secreted by baculovirus-infected insect cells. *J. Biol. Chem.* **269,** 1294–1300.
7. Sibille, J.-C., Doi, K., and Aisen, P. (1989) Hydroxyl radical formation and iron-binding proteins. Stimulation by purple acid phosphatases. *J. Biol. Chem.* **262,** 59–62.
8. Halleen, J. M., Räisänen, S., Salo, J. J., Reddy, S. V., Roodman, G. D., Hentunen, T. A., Lehenkari, P. P., Kaija, H., Vihko, P., and Väänänen, H. K. (1999) Intracellular fragmentation of bone resorption products by reactive oxygen species generated by osteoclastic tartrate-resistant acid phosphatase. *J. Biol. Chem.* **274,** 22907–22910.
9. Gaber, B. P., Sheridan, J. P., Bazer, F. W., and Roberts, R. M. (1979) Resonance Raman scattering from uteroferrin, the purple glycoprotein of porcine uterus. *J. Biol. Chem.* **254,** 8340–8342.
10. Averill, B. A., Davis, J. C., Burman, S., Zirin, T., Sanders-Löhr, J., Löhr, T. M., Sage, J. T., and Debrunner, P. G. (1987) Spectroscopic and magnetic studies of the purple acid phosphatase from bovine spleen. *J. Am. Chem. Soc.* **109,** 3760–3767.
11. Vincent, J. B., Crowder, M. W., and Averill, B. A. (1991) Spectroscopic and kinetic studies of a high-salt-stabilized form of the purple acid phosphatase from bovine spleen. *Biochemistry* **30,** 3025–3034.
12. Guddat, L. W., McAlpine, A. S., Hume, D., Hamilton, S., de Jersey, J., and Martin, J. L. (1999) Crystal structure of mammalian purple acid phosphatase. *Structure Fold. Des.* **7,** 757–767.
13. Uppenberg, J., Lindqvist, F., Svensson, C., Ek-Rylander, B., and Andersson, G. (1999) Crystal structure of a mammalian purple acid phosphatase. *J. Mol. Biol.* **290,** 201–211.
14. Lindqvist, Y., Johansson, E., Kaija, H., Vihko, P., and Schneider, G. (1999) Three-dimensional structure of a mammalian purple acid phosphatase at 2.2 Å resolution with a μ-(hydr)oxo bridged di-iron center. *J. Mol. Biol.* **291,** 135–147.
15. Sträter, N., Klabunde, T., Tucker, P., Witzel, H., and Krebs, B. (1995) Crystal structure of a purple acid phosphatase containing a dinuclear Fe(III)–Zn(II) active site. *Science* **268,** 1489–1492.
16. Klabunde, T., Sträter, N., Fröhlich, R., Witzel, H., and Krebs, B. (1996) Mechanism of Fe(III)–Zn(II) purple acid phosphatase based on crystal structure. *J. Mol. Biol.* **259,** 737–748.
17. Braman, J., Papworth, C., and Greener, A. (1996) Site-directed mutagenesis using double-stranded plasmid DNA templates. *Methods Mol. Biol.* **57,** 31–44.
18. Kaija, H., Jia, J., Lindqvist, Y., Andersson, G., and Vihko, P. (1999) Tartrate-resistant bone acid phosphatase: Large-scale production and purification of the recombinant enzyme, characterization, and crystallization. *J. Bone Miner. Res.* **14,** 424–430.
19. Vihko, P., Kurkela, R., Porvari, K., Herrala, A., Lindfors, A., Lindqvist, Y., and Schneider, G. (1993) Rat acid phosphatase: Over-expression of active, secreted enzyme by recombinant baculovirus-infected insect cells, molecular properties and crystallization. *Proc. Natl. Acad. Sci. USA* **90,** 799–803.
20. Wyckoff, M., Rodbard, D., and Crambach, A. (1977) Polyacrylamide gel electrophoresis in sodium dodecyl sulphate containing buffers using multiphasic buffer systems: Properties of the stack, valid Rf measurements and optimal procedure. *Anal. Biochem.* **78,** 459–482.
21. Bradford, M. M. (1976) A rapid and sensitive method for the quantitation of microgram quantities of protein utilizing the principle of protein–dye binding. *Anal. Biochem.* **72,** 248–254.
22. Halliwell, B., Gutteridge, J. M. C., and Aruoma, O. I. (1987) The deoxyribose method: simple "test-tube" assay for determination of rate constants for reactions of hydroxyl radicals. *Anal. Biochem.* **165,** 215–219.
23. Black, M., and Jones, M. (1983) Inorganic phosphate determination in the presence of a labile organic phosphate: Assay for carbamyl phosphate phosphatase activity. *Anal. Biochem.* **135,** 233–238.
24. Ek-Rylander, B., Flores M., Wendel, M., Heinegård, D., and Andersson, G. (1994) Dephosphorylation of osteopontin and bone sialoprotein by osteoclastic tartrate-resistant acid phosphatase. Modulation of osteoclast adhesion *in vitro*. *J. Biol. Chem.* **269,** 14853–14856.
25. Steinbeck, M., Appel, W. H., Verhoeven, A. J., and Karnovsky, M. J. (1994) NADPH-oxidase expression and *in situ* production of superoxide by osteoclasts actively resorbing bone. *J. Cell Biol.* **126,** 765–772.
26. Räisänen, S. R., Halleen, J., Parikka, V., and Väänänen, H. K. (2001) Tartrate-resistant acid phosphatase facilitates hydroxyl radical formation and colocalizes with phagocytosed *Staphylococcus aureus* in alveolar macrophages. *Biochem. Biophys. Res. Commun.* **288,** 142–150.